Ring-opening polymerization of *rac*-lactide and ε-caprolactone using zinc and calcium salicylaldiminato complexes

Joshua B. L. Gallaway, Justin R. K. McRae, Andreas Decken, and Michael P. Shaver

Abstract: Tridentate Schiff base complexes of zinc and calcium were prepared and tested in the ring-opening polymerization of ε-caprolactone and *rac*-lactide to generate biodegradable polymeric materials from biocompatible metals. Alteration of the pendant donor arm attached to the imine backbone provides some control over catalyst composition and polymerization activity. Complexes of the formula [ONN]ZnN($SiMe_3$)$_2$, where [ONN] = 2-(*N*-donor arm-imine)[4,6-di(*tert*-butyl)phenoxide], were isolated with ethyldimethylamine, ethylpiperidine, and ethylmorpholine substituents, while disproportionation led to the isolation of [ONN]$_2$Zn complexes with methylpyridine, quinoline, and ethyldiisopropylamine derivatives, two of which were crystallographically characterized. Calcium complexes were more stable and novel [ONN]CaN($SiMe_3$)$_2$ complexes with ethylpiperidine and ethyldiisopropylamine substituents were reported. Zinc and calcium catalysts coordinated to a single tridentate ligand were effective at initiating the polymerization of ε-caprolactone, but did not control the polymerizations, whereas the bis(ligand) complexes produced no polymer. These catalysts were effective at controlling the polymerization of *rac*-lactide. Coordinatively saturated complexes inhibit the polymerization, while initiation from either the amido or ligand alkoxide functionalities produces poly(lactic acid) with low polydispersities.

Key words: lactide, caprolactone, zinc, calcium, ring opening polymerization.

Résumé : On a préparé des complexes de zinc et de calcium avec des bases de Schiff tridentates et on a évalué la possibilité de les utiliser dans les polymérisations par ouverture de cycle de la ε-caprolactone et du *rac*-lactide conduisant à des matériaux polymères biodégradables à partir de produits métalliques biodégradables. L'altération du bras donneur pendant attaché au squelette de l'imine permet d'avoir un certain contrôle sur la composition du catalyseur et son activité dans la polymérisation. On a pu isoler des complexes de formule [ONN]ZnN($SiMe_3$)$_2$ (dans lesquels [ONN] = 2-(imine avec bras *N*-donneur)[4,6-di(*tert*-butyl)phénolate] portant des substituants éthyldiméthylamine, éthylpipéridine et éthylmorpholine alors qu'une disproportionation permet d'isoler les complexes [ONN]$_2$Zn avec les dérivés de la méthylpyridine, la quinoléine et l'éthyldiisopropylamine, dont deux ont été caractérisés par cristallographie. Les complexes du calcium sont plus stables et on a isolé pour la première fois les nouveaux complexes [ONN]CaN($SiMe_3$)$_2$ avec des substituants éthylpipéridine et éthyldiisopropylamine. Les catalyseurs du zinc et du calcium ne comportant qu'une coordination à un ligand tridentate sont efficaces pour initier la polymérisation de la ε-caprolactone, mais ils ne permettent pas de contrôler les polymérisations alors que les complexes avec un bis(ligand) ne permettent pas de produire des polymères. Ces catalyseurs sont efficaces pour contrôler la polymérisation du *rac*-lactide. Les complexes à coordination saturée inhibent la polymérisation alors qu'une initiation par des groupes fonctionnels amido- ou un ligand alcoolate conduisent à la production d'acide polylactique avec de faibles polydispersités.

Mots-clés : lactide, caprolactone, zinc, calcium, polymérisation par ouverture de cycle.

[Traduit par la Rédaction]

Aliphatic poly(esters) such as poly(lactic acid) (PLA) and poly(ε-caprolactone) (PCL) have gained considerable interest in recent years because of their biodegradability and renewability.[1–4] These aliphatic polymers are also bioassimilable, as hydrolysis produces nontoxic components eliminated via the Krebs cycle as CO_2 and H_2O.[3] These poly(esters) have physical properties that can be tuned and varied during polymer processing by orientation, blending, branching, cross-linking, or plasticization, enabling the application of aliphatic poly(esters) to pharmaceuticals, microelectronics, and other fields.[5,6]

PLA is an important biodegradable polymer of high industrial potential because the lactide monomer can be acquired through the fermentation of renewable resources.[3] The most common application of PCL as a biodegradable polymer involves the development of pharmaceutical drugs such as Capronor, an implanted contraceptive delivery system.[7] PCL is synthesized from the monomer ε-caprolactone, which is

Received 23 November 2011. Accepted 21 January 2012. Published at www.nrcresearchpress.com/cjc on 4 April 2012.

J.B.L. Gallaway, J.R.K. McRae, and M.P. Shaver. Department of Chemistry, University of Prince Edward Island, 550 University Avenue, Charlottetown, PEI C1A 4P3, Canada.
A. Decken. Department of Chemistry, University of New Brunswick, P.O. Box 4400, Fredericton, NB E3B 5A3, Canada.

Corresponding author: Michael P. Shaver (email: mshaver@upei.ca).

traditionally produced by the Bayer–Villiger oxidation of cyclohexanone with peracids or hydrogen peroxide[8] but can also be produced from the fermentation of starch, suggesting renewability.[9]

Aliphatic poly(esters) are commonly synthesized through ring-opening polymerization (ROP) of the corresponding cyclic ester as it offers greater control over the resulting polymers.[1–4] While ROP of lactide has been accomplished with many metals, calcium and zinc are particularly promising for industrial applications, because of their low cost, high activity, and low toxicity.[10] Ligand sets supporting active zinc and calcium lactide catalysts include β-diketiminates, tris(pyrazol) hydroborates, anilido-oxazolinates, amino-bis(pyrazol)s, N-heterocyclic carbenes, heteroscorpionates, and others.[10] The best systems offer excellent conversions over a broad temperature range and polydispersity indexes (PDIs) as low as 1.1.[10]

ROP of ε-caprolactone with calcium and zinc catalysts is comparatively understudied, although simple organic amido calcium and zinc complexes, $H_2NCaOCHMe_2$ and $Zn(N(SiMe_3)_2)_2$, show high activity and poor control.[10,11] PCL synthesis is also efficiently mediated by heterobimetallic aluminum and zinc complexes with anilido-aldimine ligands[12] and some scorpionate-derived monometallic frameworks.[10]

Inspiration for this study, however, was derived from the work of Darensbourg et al.[13–16] who showed that a series of tridentate Schiff base complexes, shown in Fig. 1, of benign metals were effective in the ROP of cyclic esters. Complexes were variably effective, with pendant dimethylamine donors coordinated to calcium providing the best activity for lactide and trimethylene carbonate, whereas zinc complexes were less effective unless substituted with bulky amino acid derived ligands and used for lactide and ε-caprolactone polymerizations.

Herein we report an extension of this series of complexes, further examining the structure/activity relationships and the role the ligand plays in controlling the ROP of *rac*-lactide and ε-caprolactone. New substitutents include diisopropylamine ($N(i\text{-}Pr)_2$), piperidine (Pip), and morpholine (Mor) functionalities. Complexes substituted with a single tridentate ligand are effective catalysts for the ROP of *rac*-lactide.

Experimental

General experimental procedures

Chemicals and solvents used for the syntheses were purchased from Sigma-Aldrich, Fisher Chemicals, and Acros Chemicals. 3,5-Di-*tert*-butyl-2-hydroxybenzaldehyde (99% pure) and starting amine reagents were all used as received. Dry solvents including tetrahydrofuran (THF), toluene, pentane, and ether were obtained from an Innovative Technology glovebox system, which was fitted with a solvent purification system. The inline purification system was made up of alumina and a copper catalyst. These anhydrous solvents were degassed by three or four freeze–pump–thaw cycles, before taking them into an MBraun LABmaster sp. glovebox. Other solvents, including $CDCl_3$, C_6D_6, and hexamethyldisiloxane, were dried over CaH_2 for at least 24 h, before vacuum transferring or vacuum distilling. The MBraun glovebox was connected to a –35 °C freezer as well as [H_2O] and [O_2] analyzers. Air-sensitive reactions involving zinc and calcium

Fig. 1. Calcium and zinc Schiff base complexes previously developed for the polymerization of cyclic esters.[13–16]

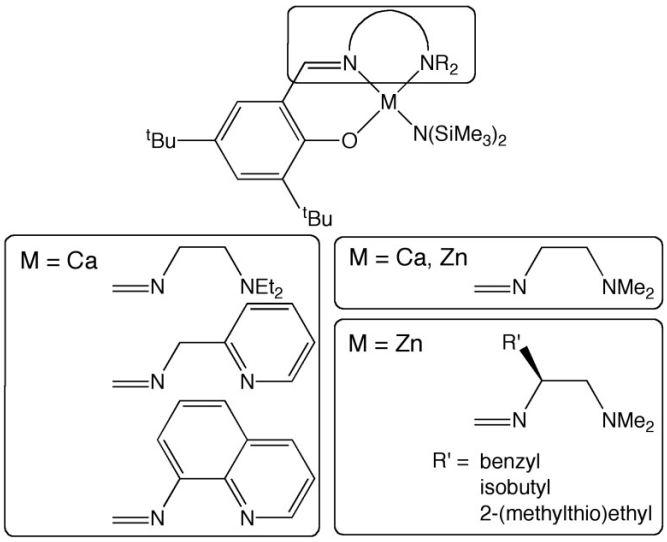

were performed under an N_2 atmosphere in the glovebox or on a Schlenk line. The Schlenk reactions utilized a dual manifold Schlenk line with Kontes valves. All samples were characterized via ^1H and ^{13}C NMR spectroscopy. These spectra were obtained by running samples on a 300 MHz Bruker Avance spectrometer. Elemental analyses were performed at Guelph Analytical Laboratories. A Bruker AXS P4/SMART 1000 diffractometer was used to obtain crystallographic data. Polymerization data were obtained using a PolymerLabs GPC50 equipped with two Jordi Gel DVB mixed bed columns (300 mm × 7.8 mm). The mobile phase used in the system was HPLC grade THF and the polymer samples were dissolved in THF to create a solution for GPC analysis, at 50 °C, at a 1 mg/mL concentration, and at a 1 mL/min flow rate. Molecular weights were measured and corrected relative to styrene standards.[17]

Synthesis and characterization

Ligand frameworks

Ligands ^{NMe_2}[ONN]ME_2 (**1**), ^{Q}[ONN] (**2**), and ^{Py}[ONN] (**3**), where ^{R}[ONN] is 2-(*N*-donor arm-imine)(4,6-di(*tert*-butyl)phenoxide, were synthesized according to a literature procedure.[14]

Synthesis of $^{N(i\text{-}Pr)_2}$[ONN]$(i\text{-}Pr)_2{}^{N(i\text{-}Pr)_2}$[ONN] ***(4)****:*

To a stirred solution of 3,5-di-*tert*-butyl-2-hydroxybenzaldehyde (2.51 g, 10.6 mmol) in methanol (25 mL) was added dropwise 2-(diisopropylamino) ethylamine (1.54 g, 10.6 mmol). The bright yellow solution was refluxed at 65 °C for approximately 10 h and then allowed to cool to room temperature. All volatiles were removed in vacuo to yield a bright yellow oil. The oil was dried under vacuum on the Schlenk line for 2 h and then purified by dissolving in cold pentane. The resulting solution was stored at –20 °C overnight, and the same purification process was repeated three times to give a dense yellow solid (1.37 g, 3.8 mmol, 36%). ^1H NMR ($CDCl_3$, ppm) δ:14.0 (1H, s, OH), 8.4 (1H, s, CH=N), 7.4–7.1 (2H, m, Ar–H), 3.6 (2H, t, J = 7 Hz, CH_2),

3.0 (2H, septet, J = 7 Hz, $CHMe_2$), 2.7 (2H, t, J = 7 Hz, CH_2), 1.5 (9H, s, $C(CH_3)_3$), 1.3 (9H, s, $C(CH_3)_3$), 1.0 (12H, d, J = 7 Hz, *i*-Pr CH_3). ^{13}C NMR ($CDCl_3$, ppm) δ: 166.3 (CH=N), 158.6, 140.0, 136.9, 126.9, 125.9, 118.1 (Ar), 61.6, 49.3, 35.2, 35.0, 34.7, 31.9, 31.8, 29.6. Elemental anal. calcd for $C_{23}H_{40}N_2O$ (%): C 76.61, H 11.18, N 7.77; found: C 76.81, H 11.11, N 7.77.

*Synthesis of ^{Pip}[ONN] (**5**):*

Ligand **5** was prepared analogously to **4**, using 3,5-di-*tert*-butyl-2-hydroxybenzaldehyde (2.56 g, 10.6 mmol), methanol (45 mL), and 4-(2-aminoethyl)piperidine (1.36 g, 10.6 mmol). This yielded a yellow powder (2.42 g, 10.6 mmol, 70%). ^{1}H NMR ($CDCl_3$, ppm) δ: 13.8 (1H, s, OH), 8.4 (1H, s, CH=N), 7.4 (1H, d, J = 2 Hz, Ar–H), 7.1 (1H, d, J = 2 Hz, Ar–H), 3.8 (2H, t, J = 7 Hz, CH_2), 2.7 (2H, t, J = 7 Hz, CH_2), 2.5 (4H, t, J = 5 Hz, CH_2), 1.6 (6H, m, CH_2), 1.5 (9H, s, $C(CH_3)_3$, 1.3 (9H, s, $C(CH_3)_3$). ^{13}C NMR ($CDCl_3$, ppm) δ: 166.75 (C=N), 158.3, 140.1, 136.9, 127.0, 126.0, 118.1 (Ar), 60.0, 57.3, 55.1, 35.4, 35.2, 34.3, 31.7, 26.2, 24.4 (CH_2). Elemental anal. calcd for $C_{22}H_{36}N_2O$ (%): C 76.69, H 10.53, N 8.13; found: C 76.90, H 10.45, N 8.10.

*Synthesis of ^{Mor}[ONN] (**6**):*

Ligand **6** was prepared analogously to **4**, using 3,5-di-*tert*-butyl-2-hydroxybenzaldehyde (2.56 g, 10.6 mmol), methanol (45 mL), and 4-(2-aminoethyl)morpholine (1.39 g, 10.6 mmol) to yield a pale yellow solid (3.82 g, 10.6 mmol, 85%). ^{1}H NMR ($CDCl_3$, ppm) δ: 13.7 (1H, s, OH), 8.4 (1H, s, CH=N), 7.4 (1H, d, J = 2 Hz, Ar–H), 7.1 (1H, d, J = 2 Hz), 3.73 (8H, t, J = 4 Hz, CH_2), 2.7 (2H, t, J = 7 Hz, CH_2), 2.5 (2H, t, J = 7 Hz, CH_2) 1.4 (9H, s, $C(CH_3)_3$), 1.3 (9H, s, $C(CH_3)_3$). ^{13}C NMR ($CDCl_3$, ppm) δ: 167.0 (C=N), 158.3, 140.2, 136.9, 127.1, 126.0, 118.1 (Ar), 67.2 (CH_2), 59.5, 57.0 (CH_2), 54.1 (CH_2), 35.2, 34.3 ($C(CH_3)_3$), 31.7, 29.6 ($C(CH_3)_3$). Elemental anal. calcd for $C_{21}H_{34}N_2O_2$ (%): C 72.79, H 9.89, N 8.08; found: C 72.84, H 9.91, N 8.15.

Zinc complexes

The complex ^{NMe_2}[ONN]ZnN$(SiMe_3)_2Me_2$ (**7**) was synthesized according to a literature procedure.[14]

*Synthesis of ^{Pip}[ONN]ZnN$(SiMe_3)_2$ (**8**):*

To a stirring solution of ^{Pip}[ONN] (2.00 g, 6.16 mmol) in THF (40 mL), a 1:1 stoichiometric ratio of $Zn(N(SiMe_3)_2)_2$ (2.38 g, 6.16 mmol) was added as a THF solution. After 2 h, the THF was removed in vacuo and the compound was isolated. To ensure complete dryness, the resulting solid was left under vacuum for several hours. To purify the solid, a pentane/toluene mixture was used to recrystallize the product. This yielded a yellow solid (1.97 g, 3.42 mmol, 58%). ^{1}H NMR ($CDCl_3$, ppm) δ: 8.2 (1H, s, CH=N), 7.4 (1H, d, J = 3 Hz, Ar–H), 6.9 (1H, d, J = 3 Hz, Ar–H), 3.7 (2H, t, J = 6 Hz, CH_2), 2.9 (2H, t, J = 6 Hz, CH_2), 2.7 (4H, t, J = 5 Hz, N–CH_2), 1.7 (6H, pentet, J = 5 Hz, CH_2), 1.5 (9H, s, $C(CH_3)_3$), 1.3 (9H, s, $C(CH_3)_3$), 0.1 (18H, s, $SiMe_3$). ^{13}C NMR ($CDCl_3$, ppm) δ: 170.1 (C=N), 167.6, 141.6, 134.7, 129.4, 128.0, 117.7 (Ar), 55.7, 55.5 (CH_2), 53.8, 52.6 (N–CH_2), 35.6, 33.8 ($C(CH_3)_3$), 31.3, 29.4 ($C(CH_3)_3$), 25.7, 23.7, 23.0 (CH_2), 5.6 ($Si(CH_3)_3$). Elemental anal. calcd for $C_{25}H_{44}N_3OSiZn$ (%): C 60.52, H 8.94, N 8.49; found: C 60.40, H 9.01, N 8.29.

*Synthesis of ^{Mor}[ONN]ZnN$(SiMe_3)_2$ (**9**):*

Complex **9** was prepared analogously to **8** using ^{Mor}[ONN] (1.01 g, 2.91 mmol), THF (40 mL), and $Zn(N(SiMe_3)_2)_2$ (1.12 g, 2.91 mmol). In contrast to **8**, **9** was mixed with 10 mL of THF and added to a stirring mixture of $Zn(N(SiMe_3)_2)_2$ in 30 mL THF. This synthesis yielded a light yellow solid (1.10 g, 1.92 mmol, 67%). ^{1}H NMR ($CDCl_3$, ppm) δ: 8.2 (1H, s, CH=N), 7.5 (1H, d, J = 3 Hz, Ar–H), 6.9 (1H, d, J = 3 Hz, Ar–H), 3.7 (4H, t, J = 6 Hz, O–CH_2), 2.9 (4H, t, J = 6 Hz, N–CH_2), 2.6 (2H, t, J = 7 Hz, CH_2), 1.9 (2H, t, J = 7 Hz, CH_2), 1.5 (9H, s, $C(CH_3)_3$), 1.3 (9H, s, $C(CH_3)_3$), 0.1 (18H, s, $SiMe_3$). ^{13}C NMR ($CDCl_3$, ppm) δ: 172.9 (C=N), 168.8, 141.7, 135.4, 130.0, 129.5, 117.2 (Ar), 68.2, 67.0 (O–CH_2), 59.0, 57.7 (CH_2), 35.8, 34.0 ($C(CH_3)_3$), 31.6, 29.7 ($C(CH_3)_3$), 5.1 ($SiMe_3$). Elemental anal. calcd for $C_{24}H_{42}N_3O_2SiZn$ (%): C 57.87, H 8.50, N 8.44; found: C 57.81, H 8.30, N 8.39.

*Synthesis of ^{Py}[ONN]$_2$Zn (**10**):*

Complex **10** was prepared analogously to **8**, leading to an impure reaction mixture. Recrystallization led to the isolation of the bis(ligand) complex in 20% yield. Altering reaction conditions to use 2 equiv of ^{Py}[ONN] (1.11 g, 3.42 mmol), THF (40 mL), and 1 equiv of $Zn(N(SiMe_3)_2)_2$ (0.66 g, 1.71 mmol) yielded a brown powder (**10**) in high yield (0.85 g, 1.54 mmol, 90%). ^{1}H NMR ($CDCl_3$, ppm) δ: 8.5 (2H, m, Ar–H), 8.2 (2H, s, CH=N), 7.3–6.8 (10H, m, Ar–H), 4.7 (4H, s, CH_2), 1.4 (18H, s, $C(CH_3)_3$), 1.3 (18H, s, $C(CH_3)_3$). ^{13}C NMR ($CDCl_3$, ppm) δ: 171.6 (C=N), 170.6, 157.1, 149.0, 141.8, 137.5, 133.5, 129.2, 129.1, 122.7, 122.3, 117.9 (Ar), 63.0 (CH_2), 35.8, 34.5 ($C(CH_3)_3$), 31.9, 29.9 ($C(CH_3)_3$). Elemental anal. calcd for $C_{42}H_{34}N_4O_2Zn$ (%): C 70.82, H 7.64, N 7.87; found: C 71.00, H 7.81, N 7.66.

*Synthesis of ^{Q}[ONN]$_2$Zn (**11**):*

Complex **11** was prepared analogously to **10** using ^{Q}[ONN] (3.00 g, 7.76 mmol), THF (40 mL), and $Zn(N(SiMe_3)_2)_2$ (1.40 g, 3.88 mmol). Complex **11** was recrystallized from a mixture of hexamethyldisiloxane and THF prior to use. The synthesis yielded a bright red solid (2.72 g, 34.6 mmol, 88%). ^{1}H NMR ($CDCl_3$, ppm) δ: 9.0 (2H, d, J = 5 Hz, Ar–H), 8.7 (2H, s, CH=N), 8.4 (2H, d, J = 5 Hz, Ar–H), 8.4–7.0 (12H, m, Ar–H), 1.6 (18H, s, $C(CH_3)_3$), 1.3 (18H, s, $C(CH_3)_3$). Elemental anal. calcd for $C_{48}H_{54}N_4O_2Zn$ (%): C 73.50, H 6.94, N 7.14; found: C 73.71, H 7.00, N 7.05.

*Synthesis of $^{N(i\text{-}Pr)_2}$[ONN]$_2$Zn(*i*-Pr)$_2$ (**12**):*

Complex **12** was prepared analogously to **10** using $^{N(i\text{-}Pr)_2}$[ONN](*i*-Pr)$_2$ (1.50 g, 4.15 mmol), THF (50 mL), and $Zn(N(SiMe_3)_2)_2$ (0.80 g, 2.07 mmol). The resulting product was a yellow solid (1.79 g, 3.02 mmol, 86%). ^{1}H NMR ($CDCl_3$, ppm) δ: 8.2 (2H, s, CH=N), 7.4 (2H, d, J = 3 Hz, Ar–H), 7.0 (2H, d, J = 3 Hz, Ar–H) 3.5 (4H, t, J = 9 Hz, CH_2), 2.9 (4H, septet, J = 4 Hz, $CH(CH_3)_2$), 2.7 (4H, t, J = 9 Hz, CH_2), 1.5 (18H, s, ($C(CH_3)_3$), 1.3 (18H, s, $C(CH_3)_3$), 0.9 (12H, d, J = 4 Hz, $CH(CH_3)_2$), 0.8 (12H, d, J = 4 Hz, $CH(CH_3)_2$). Elemental anal. calcd for $C_{46}H_{78}N_4O_2Zn$ (%): C 70.42, H 10.02, N 7.14; found: C 71.55, H 10.50, N 7.50. While repeated elemental analysis tests of isolated crystals were off, suggesting decomposition in shipping, crystals obtained from the same batch on which an X-ray diffraction

Fig. 2. Zinc complexes of Schiff base ligands.

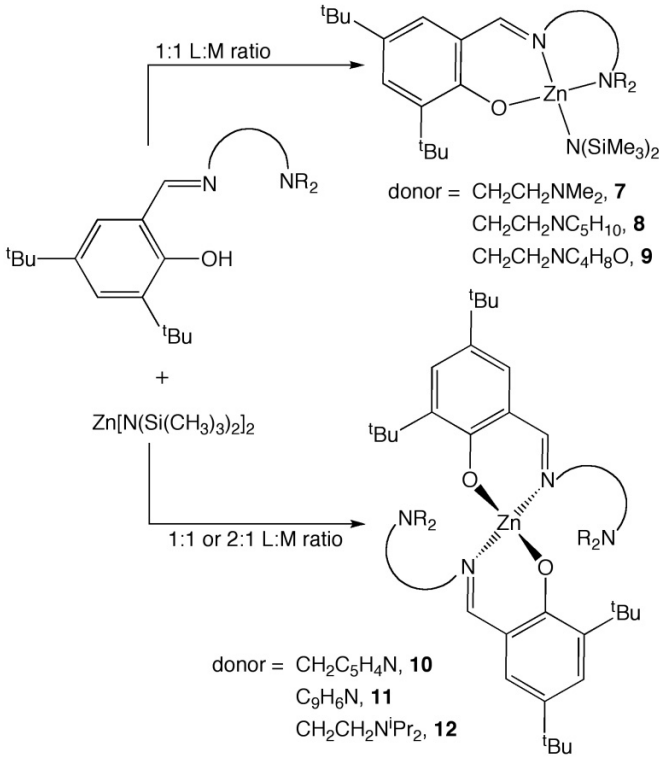

Fig. 3. Calcium complexes of Schiff base ligands.

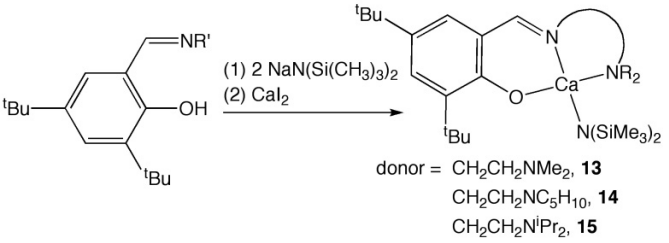

study was performed were used in the reported polymerization reactions.

Calcium complexes

^{NMe_2}[ONN]CaNMe$_2$(SiMe$_3$)$_2$ (**13**) was synthesized according to a literature procedure.[14]

*Synthesis of ^{Pip}[ONN]CaN(SiMe$_3$)$_2$ (**14**):*

^{Pip}[ONN] (0.95 g, 2.76 mmol) and NaN(SiMe$_3$)$_2$ (1.01 g, 5.5 mmol) were dissolved in THF (10 mL) and stirred at room temperature for 5 h. A stirring suspension of CaI$_2$ (0.79 g, 2.68 mmol) in THF was added dropwise to this solution and allowed to stir for 12 h. The solvent was removed in vacuo and the product was dissolved in pentane and filtered through celite. Removal of the volatiles in vacuo afforded **13** as a yellow solid (0.50 g, 9.23 mmol, 33%). ^{1}H NMR (CDCl$_3$, ppm) δ: 8.1 (1H, s, CH=N), 7.7 (1H, d, J = 3 Hz, Ar–H), 7.2 (1H, d, J = 3 Hz, Ar–H), 3.3 (2H, t, J = 6 Hz, CH$_2$), 2.1 (2H, t, J = 6 Hz, CH$_2$), 1.9 (4H, t, J = 5 Hz, CH$_2$), 1.8 (9H, s, C(CH$_3$)$_3$), 1.5 (9H, s, C(CH$_3$)$_3$), 1.2 (6H, pentet, J = 5 Hz, CH$_2$), 0.5 (18H, s, SiMe$_3$). Elemental anal. calcd for C$_{25}$H$_{44}$N$_3$CaOSi (%): C 63.78, H 9.42, N 8.93; found: C 63.70, H 9.50, N 8.62.

Fig. 4. ORTEP drawing (spheroids at 50% probability) of ^{Q}[ONN]$_2$Zn (**11**). Protons and *tert*-butyl carbons are omitted for clarity.

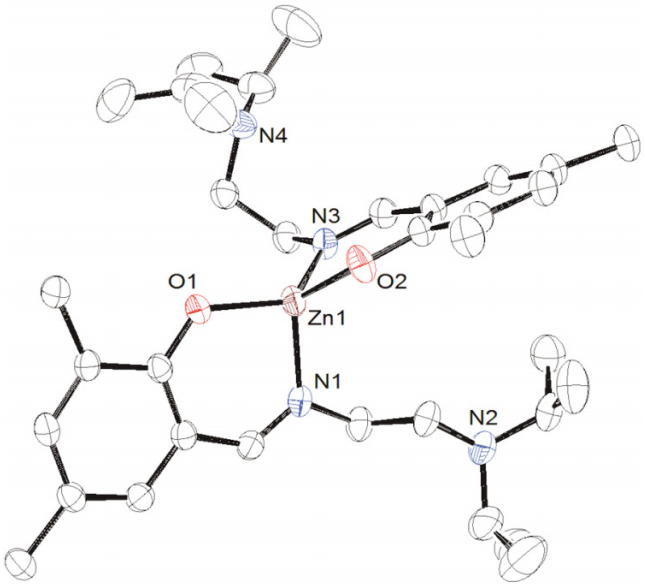

*Synthesis of $^{N(i\text{-}Pr)_2}$[ONN]CaN(SiMe$_3$)$_2$(*i*-Pr)$_2$ (**15**):*

Complex **15** was prepared analogously to **14** using 1 equiv of $^{N(i\text{-}Pr)_2}$[ONN](*i*-Pr)$_2$ (1.01 g, 2.80 mmol), 2 equiv of NaN(SiMe$_3$)$_2$ (1.03 g, 5.60 mmol), THF (30 mL), and CaI$_2$ (0.82 g, 2.80 mmol), isolating **15** as a bright yellow solid (0.80 g, 1.43 mmol, 51%). ^{1}H NMR (CDCl$_3$) δ: 8.3 (1H, s, CH=N), 7.7 (1H, d, J = 3 Hz, Ar–H), 7.2 (1H, d, J = 3 Hz, Ar–H), 3.0 (2H, septet, J = 6 Hz, CH(CH$_3$)$_2$), 2.6 (4H, m, J = 9 Hz, C*H*$_2$), 1.5 (9H, s, C(CH$_3$)$_3$), 1.4 (9H, s, C(CH$_3$)$_3$), 1.0 (12H, d, J = 6 Hz, CH(CH$_3$)$_3$), 0.3 (18H, s, SiMe$_3$). Elemental anal. calcd for C$_{26}$H$_{48}$N$_3$CaOSi (%): C 64.14, H 9.94, N 8.63; found: C 64.07, H 10.01, N 8.47.

Crystal structure analyses

Crystals of **11** and **12** were grown by vapour diffusion using pentane and toluene at –35 °C. Single crystals were coated with Paratone-N oil, mounted using a polyimide MicroMount, and frozen in the cold nitrogen stream of the goniometer. A hemisphere of data was collected on a Bruker AXS P4/SMART 1000 diffractometer using ω and θ scans with a scan width of 0.3° and 10 s (**11**) or 30 s (**12**) exposure times. The detector distance was 5 cm. The data were reduced using SAINT[18] and corrected for absorption with SADABS.[19] The structure was solved by direct methods and refined by full-matrix least-squares on F2(SHELXTL).[20] For **11**, one of the *tert*-butyl groups, attached at C(4), was disordered and the site occupancies determined using an isotropic model at 0.7 (C(9)–C(11)) and 0.3 (C(9′)–C(11′) and fixed in subsequent refinement cycles. All non-hydrogen atoms were refined using anisotropic displacement parameters. Hydrogen atoms were included in calculated positions and refined using a riding model. Graphics were created using the ORTEP program.[21]

Results and discussion

Catalyst synthesis and characterization

Tridentate Schiff base ligands were readily synthesized via

Fig. 5. ORTEP drawing (spheroids at 50% probability) of $^{N(i\text{-}Pr)_2}$[ONN]$_2$Zn(*i*-Pr)$_2$ (**12**). Protons and *tert*-butyl carbons are omitted for clarity.

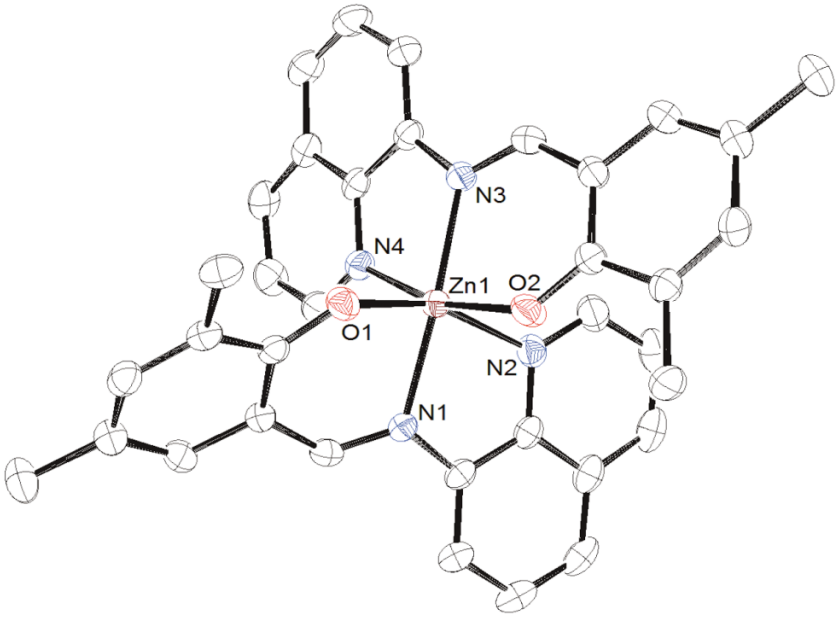

imine condensation reactions and characterized by ^{1}H and ^{13}C NMR spectroscopy (eq. [1]). Six ligands were used in this study, substituted with dimethylamine, diisopropylamine, pyridine, quinoline, piperidine, and morpholine units.

[1]

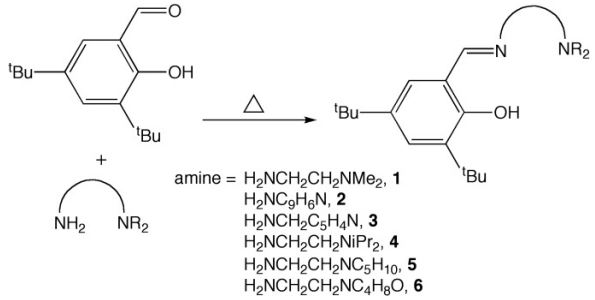

Zinc catalysts were prepared by the dropwise addition of the proligand of choice to a stirring solution of bis(bis(trimethylsilyl)amide)zinc in THF. Filtration, drying, and recrystallization from a 1:3 toluene–pentane mixture accessed the desired products. Long recrystallizations promoted a transformation from the desired ^{R}[ONN]ZnN(SiMe$_3$)$_2$ complexes, observed in crude NMR spectra, to the bis(ligand) ^{R}[ONN]$_2$Zn species. This disproportionation reaction significantly lowered isolated yields of the desired products and in some cases prevented the isolation of a pure sample of the desired ^{R}[ONN]ZnN(SiMe$_3$)$_2$ catalyst. Improved yields of the ^{R}[ONN]$_2$Zn species could be obtained from purposefully using a 2:1 ligand–metal ratio. Ligands **1**–**6** and isolated complexes **7**–**12** are shown in Fig. 2. Complex formation was readily identified by a diagnostic shift in the imine resonance to δ 8.2 for alkyl-substituted nitrogen donor arms and δ 8.5 and 8.7 for pyridyl and quinolynyl donor arms, respectively, as well as the disappearance of the hydroxy signals. The integration and presence of N(SiMe$_3$)$_2$ protons at δ 0.1 was diagnostic for the formation of mono- or bis-ligated complexes.

Table 1. Selected bond distances (Å) and angles (°) for ^{Q}[ONN]$_2$Zn (**11**) and $^{N(i\text{-}Pr)_2}$[ONN]$_2$Zn (**12**).

	Complex	
	11	**12**
Bond distance (Å)		
Zn(1)–O(1)	2.0260(15)	1.9081(12)
Zn(1)–O(2)	2.0016(15)	1.9106(13)
Zn(1)–N(1)	2.1047(16)	2.0099(16)
Zn(1)–N(2)	2.2730(19)	—
Zn(1)–N(3)	2.1025(17)	2.0018(16)
Zn(1)–N(4)	2.2365(18)	—
Bond angle (°)		
O(1)–Zn(1)–N(1)	86.20(6)	95.08(6)
O(1)–Zn(1)–N(2)	158.42(6)	—
N(1)–Zn(1)–N(2)	75.36(7)	—
O(2)–Zn(1)–N(3)	88.52(6)	96.15(6)
O(2)–Zn(1)–N(4)	163.54(6)	—
N(3)–Zn(1)–N(4)	76.20(7)	—
(O1)–Zn(1)–O(2)	91.00(6)	113.69(6)

Calcium complexes were prepared via the ^{R}[ONN] sodium salt with 1 equiv of ligand and 2 equiv of NaN(SiMe$_3$)$_2$ reacted for 5 h in THF followed by dropwise addition of CaI$_2$ to the reaction mixture. Removal of solvent after 12 h followed by filtration and recrystallization from pentane afforded three desired complexes of the form ^{R}[ONN]CaN(SiMe$_3$)$_2$ characterized by ^{1}H and ^{13}C NMR spectroscopy (**13**–**15**, Fig. 3). Yields were moderate compared with the corresponding Zn complexes, potentially because of the relative stability of the CaI$_2$. Attempts to improve yields with longer reaction times and higher temperatures were unsuccessful and led to complex decomposition. Of note, pyridine and quinoline functionalities were not employed as the complexes had been previously tested, whereas morpholine substituents promoted the formation of an intractable mixture of solids. Again, the complex formation was noted in spectroscopic

Table 2. Selected crystallographic data and refinement details for $^{Q}[ONN]_2Zn$ (**11**) and $^{N(i\text{-}Pr)_2}[ONN]_2Zn$ (**12**).

	Complex	
Crystallographic parameters	**11**	**12**
Empirical formula	$C_{48}H_{54}N_4O_2Zn$	$C_{46}H_{78}N_4O_2Zn$
Formula mass	784.32	784.49
Colour, habit	Orange, rod	Colourless, rod
Dimensions (mm)	0.60×0.10×0.05	0.60×0.30×0.25
Crystal system	Triclinic	Monoclinic
Space group	*P*-1	*P*2(1)/*c*
Z	2	4
a, *b*, *c* (Å)	10.1627(17), 13.790(2), 16.511(3)	11.0836(13), 14.8067(18), 28.774(3)
α, β, γ (°)	104.350(2), 104.649(2), 99.769(2)	90, 93.411(2), 90
V (Å^3)	2101.1(6)	4713.7(10)
Temperature (K)	188(1)	188(1)
D_{calcd} (Mg m^{-3})	1.240	1.105
Radiation	Mo Kα	Mo Kα
μ (mm^{-1})	0.627	0.558
F(000)	832	1712
Reflections (obs.)	13846	32145
Reflections (ind.)	8955	10552
Data/restr./param.	8955 / 15 / 520	10552 / 0 / 498
Theta range (°)	1.57–27.49	1.42–27.50
Goodness-of-fit	1.052	1.027
R_1, wR_2	0.0413, 0.0822	0.0369, 0.0872
Largest peak/hole (e A^{-3})	0.330, –0.518	0.284, –0.275

studies by a shift in the imine resonance, the disappearance of hydroxyl resonances, and the presence and integration of $N(SiMe_3)_2$ signals.

Crystals suitable for X-ray diffraction studies were grown for **11** and **12** by vapour diffusion of pentane into toluene. The crystal structure of **11** (Fig. 4) indicates the complex has a distorted octahedral geometry with coordination of the quinoline nitrogens to afford a formally 22-electron complex. This six-coordinate complex, with both tridentate ligands arranged in a meridional geometry, contrasts with similar four-coordinate diphenolato complexes synthesized by Zhang et al.[23] In **11**, Zn–N bonds ranging from 2.10 to 2.27 Å contrast with the stronger Zn–O bonds of 2.00 and 2.03 Å. The structure of **12**, however, shows the Zn centre in a distorted T_d geometry (Fig. 5), similar to a previously published bidentate salicylaldimine structure.[23] A four-coordinate structure is favoured, correlating with the removal of the electron-withdrawing quinoline ring structure and the increased steric hindrance of the isopropyl substituents. As expected, the complex has shorter Zn–O (1.91 Å) and Zn–N (2.00, 2.01 Å) bond lengths compared with **11**. Selected bond distances, bond angles, and crystallographic parameters are provided in Tables 1 and 2.

Ring-opening polymerizations of *rac*-lactide and ε-caprolactone — Screening reactions

Polymerizations of ε-caprolactone mediated by complexes **7**–**15** are summarized in Table 3. Polymerizations with monomer–catalyst ratios of 100:1 were carried out in toluene (3 mL) at room temperature. No additional alcohol initiator was added to the reactions, so initiation from latent trimethylsilylamide or ligand alkoxide functionalities was expected. Temperatures were maintained at room temperature as higher temperatures and bulk polymerization led to significant transesterification and broadened molecular weight distributions, contrasting previous reports,[15,21] but supporting the poor activity of previously reported chiral variants.[22] None of the catalysts were effective at controlling the polymerization, however, certain trends can be highlighted. Complexes with a single ligand and bis(trimethylsilyl)amido initiating group initiate a productive PCL polymerization, however, polydispersities (PDIs) are high and observed molecular weights are higher than expected from monomer conversion. Complexes with two ligands, lacking the amido functionality, are unable to initiate the polymerization. The calcium complexes are significantly faster at polymerizing the ε-caprolactone monomer. Chromatographic analysis of these polymers still suggests a lack of control over this reaction, with multimodal molecular weight distributions. While disproportionation is possible for the monoligated complexes under polymerization conditions, which may explain the lack of control, no disproportionation was observed for **7**–**9** or **13**–**15** in coordinating solvents.

Polymerizations of *rac*-lactide mediated by complexes **7**–**15** are summarized in Table 4. Reactions were carried out at 70 °C in toluene for 30 or 240 min depending upon the observed reactivity of the complexes. Clear trends in catalyst performance are observed. Complexes **7**–**9**, ligated by a single tridentate ligand, produce PLAs of predictable molecular weights and low polydispersities. The fastest catalyst, capable of polymerizing nearly 100 equiv of *rac*-lactide in under 30 min, is the previously reported **7**, substituted with a sterically unencumbered dimethylamine donor arm. Increasing the steric bulk slows the polymerization, as expected. Both the rate of polymerization and the control of the polymerization are inhibited by the morpholine ligand, suggesting the pendant oxygen of the morpholine ring may block lactide coordination and ROP. Bis(ligand) complexes also initate and control the polymerization of lactide, likely inserting into one

Table 3. Polymerization of ε-caprolactone (ε-CL) mediated by complexes **7**–**15**.

[I]	Time (min)	Conv. (%)	M_n	$M_{n,th}$[a]	PDI
7	120	54	37898	6324	1.71
8	120	72	25150	8378	1.72
9	120	28	51714	3356	1.79
10	360	0	na	na	na
11	360	0	na	na	na
12	360	0	na	na	na
13	15	68	32841	7922	1.73
14	15	81	21544	9406	1.80
15	15	72	32583	8218	1.72

Note: Reactions carried out at 25 °C in 3 mL of toluene with monomer:catalyst ratios of 100:1. Molecular weights corrected for changes in relative retention times versus styrene standards. [I], initiator; M_n, number average molecular weight; $M_{n,th}$, theoretical molecular weight; PDI, polydispersity index; na, not available.

[a] $M_{n,th}$ = % conversion × MW ε-CL × 100 + MW $N(SiMe_3)_2$.

Table 4. Polymerization of *rac*-lactide mediated by complexes **7–15**.

[I]	Time (min)	Conv. (%)	M_n	$M_{n,th}$[a]	PDI
7	30	86	10079	12556	1.25
8	30	61	7374	8952	1.28
9	30	48	6338	7079	1.61
10	240	94	20508	13872	1.39
11	240	0	na	na	na
12	240	98	19878	14484	1.31
13	240	54	8321	7943	1.20
14	240	47	5987	6934	1.20
15	240	58	8986	8520	1.12
15[b]	400	58	18007	17040	1.25
15[c]	620	58	31998	34080	1.34

Note: Reactions carried out at 70 °C in 3 mL of toluene with monomer–catalyst ratios of 100:1. Molecular weights corrected for changes in relative retention times versus styrene standards. [I], initiator; M_n, number average molecular weight; $M_{n,th}$, theoretical molecular weight; PDI, polydispersity index; na, not available.

[a] $M_{n,th}$ = % conversion × MW *rac*-LA × 200 + MW initiating group.

[b] Ratio of 200:1 monomer–catalyst used.

[c] Ratio of 400:1 monomer–catalyst used.

of the zinc alkoxide bonds to the ligand.[23,24] Molecular weights were higher than theoretical, suggesting not all ligands may initiate the polymerization. Interestingly, the quinoline-substituted complex, which in the solid state had no open coordination sites, is completely unreactive towards lactide even at higher temperatures and longer reaction times, suggesting this octahedral coordination mode may be maintained in solution. No shift in lactide or catalyst resonances are noted in ^{1}H NMR spectra of 1:1 mixtures of **11** and *rac*-lactide, supporting this statement.

Finally, the calcium complexes prepared were all effective in the polymerization of *rac*-lactide, with similar levels of control regardless of the nature of the pendant donor arm. Reactions were slow, however, requiring longer reaction times to achieve higher conversions. Due to the inferior quality of the catalysts compared with industry standards, full reaction kinetics were not pursued. However, further evidence of polymerization control is offered by variation of [M]:[I] (monomer to initiator) ratios, as shown in Table 4 for catalyst **15**. When polymerizations are quenched at the same conversion, molecular weights increase linearly and correlate well with predicted values. A slight increase in PDI at longer reaction times suggest the catalysts may have limited thermal stability. All catalysts produced atactic PLA and showed no stereospecificity. Interestingly, the calcium complexes show lower activity, potentially because of their larger size and lower Lewis acidity, contributing to a lower overall reactivity.

Conclusions

Nine zinc and calcium complexes supported by phenoxy-imine ligands with various pendant donors were prepared, characterized, and screened as catalysts in the ROP of ε-caprolactone and *rac*-lactide. Seven of these catalysts are novel and include pendant piperidine, morpholine, diisopropylamine, pyridine, and quinoline donors to compare with first-generation catalysts substituted with dimethylamine donors. Zinc complexes have a tendency to disproportionate to form bis(ligand) species, which are ineffective for the polymerization of ε-caprolactone but initiate slowly to produce PLAs of controlled PDIs and molecular weights. Improved control was achieved through the use of zinc and calcium complexes coordinated to a single ligand framework with low PDI.

Acknowledgement

We thank the Natural Sciences and Engineering Research Council of Canada (NSERC) and the University of Prince Edward Island, Charlottetown, for financial support, and the Canada Foundation for Innovation and the Atlantic Canada Opportunities Agency for infrastructure. We would also like to thank NSERC for Undergraduate Student Research Awards to Justin McRae and Josh Gallaway.

References

(1) Stanford, M. J.; Dove, A. P. *Chem. Soc. Rev.* **2010**, *39* (2), 486. doi:10.1039/b815104k.
(2) Cameron, D. J. A.; Shaver, M. P. *Chem. Soc. Rev.* **2011**, *40* (3), 1761. doi:10.1039/c0cs00091d.
(3) Dove, A. P. *Chem. Commun. (Camb.)* **2008**, (48): 6446. doi:10.1039/b813059k.
(4) Dechy-Cabaret, O.; Martin-Vaca, B.; Bourissou, D. *Chem. Rev.* **2004**, *104* (12), 6147. doi:10.1021/cr040002s.
(5) Sinclair, R. G. *J. Macromol. Sci. Pure Appl. Chem.* **1996**, *A33* (5), 585. doi:10.1080/10601329608010880.
(6) Davis, K. A.; Burdick, J. A.; Anseth, K. S. *Biomaterials* **2003**, *24* (14), 2485. doi:10.1016/S0142-9612(02)00582-3.
(7) Dumitriu, S. *Polymeric Biomaterials;* Marcel Dekker: New York, 2002; Chapter 4.
(8) Arbaoui, A.; Redshaw, C. *Polym. Chem.* **2010**, *1* (6), 801. doi:10.1039/b9py00334g.
(9) Minami, M.; Kozaki, S. Method for Producing Aliphatic Polyester. U.S. Patent Appl. Publ. 20030023026 A1 20030130, 2003.
(10) Hayes, P. G.; Wheaton, C. A.; Ireland, B. J. *Dalton Trans.* **2009**, (25), 4832. doi:10.1039/b819107g.

(11) Tang, H.-Y.; Chen, H.-Y.; Huang, J.-H.; Lin, C.-C. *Macromolecules* **2007**, *40* (25), 8855. doi:10.1021/ma071540k.
(12) Gao, A.-H.; Yao, W.; Mu, Y.; Gao, W.; Sun, M.-T.; Su, Q. *Polyhedron* **2009**, *28* (13), 2605. doi:10.1016/j.poly.2009.05.037.
(13) Darensbourg, D. J.; Choi, W.; Richers, C. P. *Macromolecules* **2007**, *40* (10), 3521. doi:10.1021/ma062780n.
(14) Darensbourg, D. J.; Choi, W.; Karroonnirun, O.; Bhuvanesh, N. *Macromolecules* **2008**, *41* (10), 3493. doi:10.1021/ma800078t.
(15) Darensbourg, D. J.; Karroonnirun, O. *Inorg. Chem.* **2010**, *49* (5), 2360. doi:10.1021/ic902271x.
(16) Darensbourg, D. J.; Karroonnirun, O. *Macromolecules* **2010**, *43* (21), 8880. doi:10.1021/ma101784y.
(17) Kowalski, A.; Duda, A.; Penczek, S. *Macromolecules* **1998**, *31* (7), 2114. doi:10.1021/ma971737k.
(18) SAINT 7.23A. Bruker AXS, Inc., Madison, WI, 2006.
(19) Sheldrick, G. SADABS. Bruker AXS, Inc., Madison, WI, 2008.
(20) Sheldrick, G. M. *Acta Crystallogr.* **2008**, *A64* (1), 112. doi:10.1107/s0108767307043930.
(21) Farrugia, L. J. *J. Appl. Cryst.* **1997**, *30* (5), 565. doi:10.1107/S0021889897003117.
(22) Labourdette, G.; Lee, J.-C. D.; Patrick, B. O.; Ezhova, M. B.; Mehrkhodavandi, P. *Organometallics* **2009**, *28* (5), 1309. doi:10.1021/om800818v.
(23) Zhang, C.; Wang, Z.-X. *J. Organomet. Chem.* **2008**, *693* (19), 3151. doi:10.1016/j.jorganchem.2008.07.002.
(24) Bhunora, S.; Mugo, J.; Bhaw-Luximon, A.; Mapolie, S.; Van Wyk, J.; Darkwa, J.; Nordlander, E. *Appl. Organomet. Chem.* **2011**, *25* (2), 133. doi:10.1002/aoc.1728.